



## Accepted Article

**Title:** SnO<sub>2</sub>-based catalysts with low temperature performance for oxidative coupling of methane: insight into the promotional effects of alkali metal oxides

**Authors:** Liang Peng, Junwei Xu, Xiuzhong Fang, Wenming Liu, Xianglan Xu, Liang Liu, Zhongchen Li, Renyang Zheng, and Xiang Wang

This manuscript has been accepted after peer review and appears as an Accepted Article online prior to editing, proofing, and formal publication of the final Version of Record (VoR). This work is currently citable by using the Digital Object Identifier (DOI) given below. The VoR will be published online in Early View as soon as possible and may be different to this Accepted Article as a result of editing. Readers should obtain the VoR from the journal website shown below when it is published to ensure accuracy of information. The authors are responsible for the content of this Accepted Article.

**To be cited as:** *Eur. J. Inorg. Chem.* 10.1002/ejic.201701440

**Link to VoR:** <http://dx.doi.org/10.1002/ejic.201701440>

# SnO<sub>2</sub>-based catalysts with superior low temperature performance for oxidative coupling of methane: insight into the promotional effects of alkali metal oxides

Liang Peng,<sup>[a]</sup> Junwei Xu,<sup>[a]</sup> Xiuzhong Fang,<sup>[a]</sup> Wenming Liu,<sup>[a]</sup> Xianglan Xu,<sup>[a]</sup> Liang Liu,<sup>[a]</sup> Zhongchen Li,<sup>[a]</sup> Renyang Zheng,<sup>[b]</sup> Xiang Wang<sup>\*,[a]</sup>

**Abstract:** To develop reactive catalysts for oxidative coupling of methane at low temperature, different alkali metal oxides have been adopted to modify the surface of SnO<sub>2</sub> in this study. In comparison with the un-modified SnO<sub>2</sub>, the reaction performance of all the modified catalyst can be significantly improved, among which lithium oxide shows the best promotional effects, and the optimal catalyst was achieved with a Sn/Li molar ratio of 5/5. Over this catalyst, the highest C<sub>2</sub> product yield of 16 % has been achieved at 750 °C. XPS and CO<sub>2</sub>-TPD results have revealed that for those catalysts with evident enhanced OCM reaction performance, the co-existence of suitable amount of surface alkaline and electrophilic oxygen sites is indispensable. Furthermore, over the catalysts modified by different amount of lithium oxide, the C<sub>2</sub> yield at different temperatures is nearly proportional to the amounts of both surface intermediate alkaline sites and electrophilic oxygen species. Therefore, it is concluded that the abundance and the concerted interaction of these two types of surface active sites are the major factors determining the reaction performance of the SnO<sub>2</sub>-based catalysts. Last but not the least, the optimized catalyst, which has a Sn/Li molar ratio of 5/5 and also contains equal amounts of SnO<sub>2</sub> and Li<sub>2</sub>SnO<sub>3</sub> crystalline phases, exhibits much better reaction performance than Mn/Na<sub>2</sub>WO<sub>4</sub>/SiO<sub>2</sub>, the most promising catalyst at present, at low temperature region (below 750 °C). After all, this may give people some new insight into developing novel type of OCM catalysts that can be operated at low temperature and facilitate the industrialization process of this important chemical engineering reaction.

## Introduction

Due to the fast consumption of crude oil, much attention has been transferred to the utilization of abundant natural gas, which usually consists of 83 % ~ 99 % methane.<sup>[1-2]</sup> Over the past decades, both the direct and indirect ways to convert methane into value-added chemical products have been intensively investigated.<sup>[3]</sup> The typical indirect ways include methane steam reforming, dry reforming and partial oxidation, during which, methane is first converted into syngas, and then synthesized into higher value hydrocarbons by Fischer-Tropsch reaction.<sup>[3]</sup> The typical direct ways include non-oxidative methane conversion to aromatics,<sup>[4-5]</sup> and oxidative coupling of methane (OCM) to C<sub>2</sub> hydrocarbons.<sup>[6-10]</sup> For indirect conversion of methane, multiple steps are required, which obviously makes the technological process more complicated. Therefore,

developing catalysts to directly convert methane into hydrocarbons with higher value is desirable and have been paid much attention. Catalytic oxidative coupling of methane to higher hydrocarbons is regarded as an effective direct way to utilize methane, which has aroused great interest around the world over recent ten years.

Since Keller and Bhasin first reported their work on OCM in early 1980s,<sup>[6-8, 10-15]</sup> a lot of work on screening active and selective catalysts have been performed. The investigated catalysts can be divided roughly into two groups, the non-redox and the redox type. As a typical example for the non-redox type catalysts, Li/MgO catalysts have been reported to be effective for the reaction,<sup>[16-18]</sup> on which the surface alkaline sites and oxygen species are regarded to be the active sites.<sup>[3, 19-22]</sup> However, Li/MgO catalysts still suffer from deactivation due to the vaporization of Li<sup>+</sup> cations.<sup>[23]</sup> As a typical example for the redox type catalysts, Mn-Na<sub>2</sub>WO<sub>4</sub>/SiO<sub>2</sub> catalysts have been tremendously studied over past 30 years.<sup>[24-30]</sup> Reducible metal oxides can store and release oxygen cyclically between multiple valence states.<sup>[19]</sup> The surface lattice oxygen (O<sup>2-</sup>) has been proposed to be the active sites for the OCM.<sup>[20]</sup> Whereas, for both groups of catalysts, surface electrophilic oxygen species (O<sup>-</sup>, O<sub>2</sub><sup>-</sup> and O<sub>2</sub><sup>2-</sup>) are believed to be crucial for the reaction and could decide the selective formation of the coupling products.<sup>[3, 31-34]</sup> Up to date, Mn-Na<sub>2</sub>WO<sub>4</sub>/SiO<sub>2</sub> and Li/MgO have been reported to be the most promising catalysts for OCM reaction.<sup>[17, 27, 35-36]</sup> Unfortunately, over both of the two catalysts, the one way C<sub>2</sub> product yield is still below 30%, which is regarded as the lowest yield requirement for the industrialization of this reaction.<sup>[20, 26]</sup> In addition, on both types of catalysts, it generally requires high temperature above 750 °C to proceed the reaction effectively, though some interesting work has been reported recently to decrease the reaction temperature over Mn-Na<sub>2</sub>WO<sub>4</sub>/SiO<sub>2</sub> catalyst evidently.<sup>[28, 36]</sup> Therefore, there is still strong incentive to find more reactive and selective catalysts to overcome these disadvantages.

It is usually accepted that for a good OCM catalyst, suitable alkaline sites, selective oxygen sites and high thermal stability are required.<sup>[19]</sup> The abstraction of the first hydrogen atom from a CH<sub>4</sub> molecule on an active oxygen site or a basic oxygen site is considered as the first and rate-determining step.<sup>[19, 37-38]</sup> Then the formed methyl radicals either diffuse to the gas phase to couple with each other to form C<sub>2</sub>H<sub>6</sub>, or stay on the surface to be oxidized further into CO<sub>2</sub> and CO. As a secondary product, C<sub>2</sub>H<sub>4</sub> is formed by C<sub>2</sub>H<sub>6</sub> dehydrogenation on the surface of the catalysts. The hydrogen abstraction process produces hydroxyl groups, which react with each other to form water and generate oxygen vacancies at the same time. The surface oxygen vacancies will then be restored by the gas phase O<sub>2</sub>.

Tin dioxide is an n-type semiconductor, which contains abundant metastable surface deficient oxygen species and its lattice oxygen is also reducible and reactive.<sup>[39-42]</sup> In addition, its melting point is as high as 1630 °C,<sup>[43]</sup> testifying that it has both good chemical and thermal stability. Tin dioxide has been

[a] L Peng, X Fang, J Xu, W Liu, X Xu, Z Fu, H Peng, X Wang. Institute of Applied Chemistry, College of Chemistry, Nanchang University, Nanchang, 330031, P. R. China

[b] R. Zheng. Research Institute of Processing(RIIP), SINOPEC, 18 Xueyuan Road Haidian district, Beijing 100083, China

\* Corresponding author, E-mail: [xwang23@ncu.edu.cn](mailto:xwang23@ncu.edu.cn) (X. Wang).

reported previously to be very good oxidation catalysts,<sup>[44-48]</sup> especially after its lattice matrix is doped with secondary metal cations to form solid solution structures, as found by this group.<sup>[49-50]</sup> Nevertheless, SnO<sub>2</sub> related catalysts have been rarely used for the oxidative coupling of methane, and SnO<sub>2</sub> is mainly adopted as a catalyst additive.<sup>[3, 21]</sup> Based on the above mentioned former studies, it is postulated that by using alkali metal oxides to tune the surface of SnO<sub>2</sub>, catalytic materials with both abundant alkaline sites and redox sites might be achieved, which could match well the active site requirements for an effective OCM catalysts.

Therefore, to develop more efficient catalysts that can be operated at lower temperature and to investigate the influence of alkali metal oxides on the reaction performance of SnO<sub>2</sub>, in this work, different alkali metal oxides have been adopted to modify SnO<sub>2</sub> to prepare catalysts for OCM reaction. It has been revealed that in comparison with the un-modified SnO<sub>2</sub>, all the modified catalysts demonstrate significantly improved performance for the target reaction due to the concerted interaction between the alkaline sites and the electron deficient oxygen species. Lithium oxide displays the best promotion effects among all the alkali metal oxides, on which the highest C<sub>2</sub> product yield of 16 % can be obtained by adjusting an appropriate Sn/Li molar ratio. It is particularly mentioned here that the optimal catalysts also exhibits much better reaction performance than Mn-Na<sub>2</sub>WO<sub>4</sub>/SiO<sub>2</sub>, the most promising catalyst at present, at low temperature region between 650-700 °C, which could give people some new insights on how to develop catalysts that can be operated at low temperatures. With different characterization methods, the relationship between the reaction performance and the structure of the catalysts has been elucidated.

## Results and Discussion

### Reaction performance of the catalysts modified by different alkali metal oxides

The reaction performance of the catalysts modified by different alkali metal oxides has been evaluated for oxidative coupling of methane, with the results demonstrated in Figure. 1. Compared with the un-modified SnO<sub>2</sub> support, the addition of alkali metal oxides obviously increases the CH<sub>4</sub> conversion, C<sub>2</sub> product selectivity and yield over all the modified catalysts. With the increasing of the reaction temperature from 650 to 750 °C, the CH<sub>4</sub> conversion, C<sub>2</sub> product selectivity and yield improve slightly, testifying that the reaction performance of these SnO<sub>2</sub>-based catalysts is not sensitive to the reaction temperatures. It is mentioned here that though Sn9Na1, the catalyst modified by sodium oxide, has the highest initial CH<sub>4</sub> conversion, C<sub>2</sub> product selectivity and yield among all the catalysts, they decay gradually with the increasing of the temperature, indicating its surface active sites are not as stable as those on other catalysts. Comparing the stable reaction performance above 700 °C, the CH<sub>4</sub> conversion, C<sub>2</sub> product selectivity and yield follow the sequence of Sn9Li1 > Sn9Cs1 > Sn9K1 > Sn9Na1 > SnO<sub>2</sub>. This testifies strongly that all the alkali metal oxides have evident promotion effects on SnO<sub>2</sub> for oxidative coupling of methane but with different extents, among which lithium oxide displays the best enhancement effect.

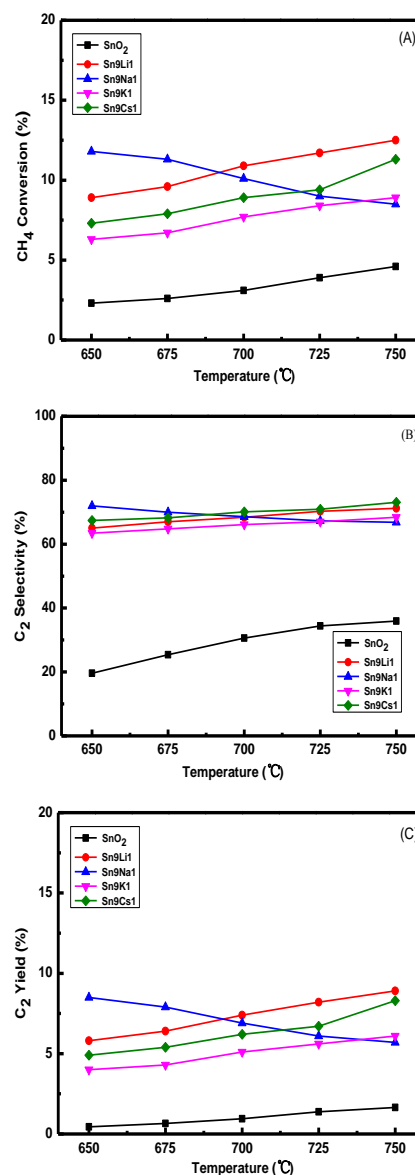


**Figure 1.** Reaction performance of the catalysts modified by different alkali metal oxides. (A) CH<sub>4</sub> conversion, (B) C<sub>2</sub> product selectivity, (C) C<sub>2</sub> product yield. Reaction conditions: cat 0.2g, CH<sub>4</sub>/O<sub>2</sub>=4:1, GHSV=18000mLh<sup>-1</sup>, 50% Nitrogen balanced.

### XRD and N<sub>2</sub>-BET measurements of the catalysts modified by different alkali metal oxides

The phase composition of the catalysts was analyzed by XRD techniques, with the patterns displayed in Figure. 2. For all the modified catalysts, similar to the un-modified SnO<sub>2</sub> support, tetragonal rutile SnO<sub>2</sub> is the only crystalline phase detected. No any diffraction feature related to alkali metal oxides can be observed. Taking into account of the fact that all the catalysts were prepared with the traditional impregnation method, it is believed that after calcination the formed alkali metal oxides are dispersed finely on the surface of the SnO<sub>2</sub> support, thus escaping the detection by XRD.<sup>[51]</sup>

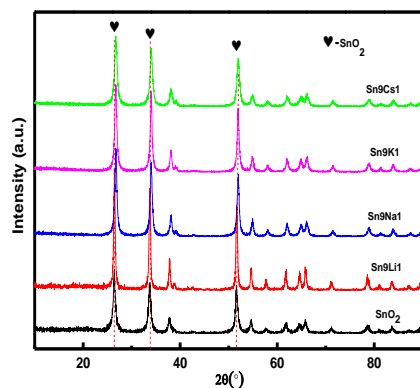


**Figure 2.** XRD patterns of the catalysts modified by different alkali metal oxides.

The texture properties of the catalysts were analysed by means of  $N_2$  adsorption-desorption technique, with the results displayed in Table 1. As shown in Figure. S1, all the catalysts exhibit typical type V isotherms with a capillary condensation step, proving the presence of mesoporous structure. The hysteresis loop in the relative pressure ( $P/P_0$ ) range of 0.6-1.0 belongs to H3-type, which is typical for the presence of inter-particle meso-pores, in line with the mono-modal pore distribution profiles in Figure. S1 (B). As indicated in Table 1, after the addition of alkali metal oxides, the pore volumes of the catalysts decrease more or less in comparison with the individual  $SnO_2$  support, implying the blockage of some initial pores. While the average pore diameters of the two catalysts modified by lithium and sodium oxides have little change, the other two samples modified by potassium and cesium oxides have some evident decrease. Moreover, compared with pure  $SnO_2$  support, the surface areas of all the modified catalysts is also nearly intact. All these experimental facts testify that the addition of different alkali metal oxides with a 9/1 molar ratio has little alteration on the texture properties of the catalysts, and which should not be the major reason influencing the reaction performance of the catalysts.

**Table 1.** Physical-chemical properties of the catalysts modified by different alkali metal oxides

Sample	$S_{BET}$ ( $m^2/g$ )	Pore volume ( $cm^3/g$ )	Pore diameter (nm)
$SnO_2$	12	0.73	10.0
$Sn9Li1$	13	0.72	9.9
$Sn9Na1$	12	0.50	10.3
$Sn9K1$	11	0.60	9.0
$Sn9Cs1$	9	0.61	8.8

### XPS study on the catalysts modified by different alkali metal oxides

XPS was used to investigate the surface properties of the catalysts modified by different alkali metal oxides, with the spectra shown in Figure. 3 and S2. Figure. S2(A) testifies that all the alkali metals are fully oxidized with a valence state of +1;

and Figure. S2(B) proves that Sn is fully oxidized as  $Sn^{4+}$ , in agreement with the XRD results.

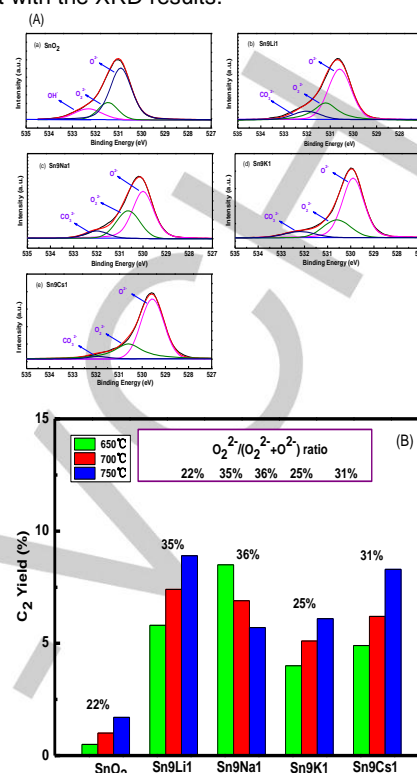


**Figure 3.** XPS analysis of the surface oxygen properties for the catalysts modified by different alkali metal oxides

To understand the surface oxygen properties of the catalysts, the O 1s spectra of the catalysts have been analyzed in detail, with the quantified results listed in Table 2. As shown in Figure. 3(A), all the catalysts displays bi-modal O 1s peaks, indicating the presence of surface oxygen species with different chemical environments. According to the former publications, the major O 1s peak at approximately 530.0 eV can be assigned to the surface lattice oxygen species ( $O^{2-}$ ); and the shoulder peak above 532.0 eV is believed to be composed of the loosely bonded surface oxygen species.<sup>[52-53]</sup> For pure  $SnO_2$ , surface hydroxyl groups are generally present.<sup>[54-55]</sup> In contrast, for the samples modified by alkali metal oxides, the formation of carbonate is observed, as proved by Figure. S2(C). Based on these findings, the O 1s peaks of the catalysts have been deconvoluted and fitted, with the detailed results summarized in Table 2. It is revealed that an electron deficient oxygen species,  $O_2^{2-}$ , is detected on the surface of all the catalysts. Former reports have testified that several types of surface electrophilic oxygen species ( $O^-$ ,  $O_2^-$  and  $O_2^{2-}$ ) are critical for the selective formation of the coupling products.<sup>[31-32, 34, 37]</sup> Therefore, by subtracting the contribution from hydroxyl group on pure  $SnO_2$  and the contribution from carbonate on other modified samples, the  $O_2^{2-}/(O_2^{2-}+O_2^-)$  molar ratios of the catalysts have been quantified in Table 2. Apparently, after modification by alkali metal oxides,  $O_2^{2-}/(O_2^{2-}+O_2^-)$  molar ratio of each sample increases in comparison with that of the individual  $SnO_2$ , indicating the formation of more mobile and selective oxygen species.

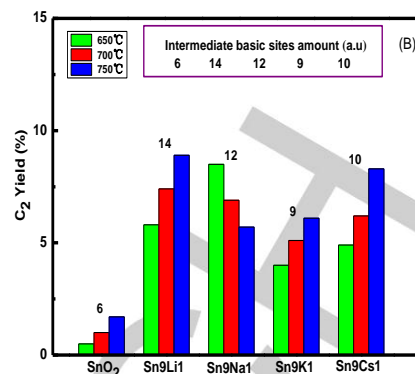
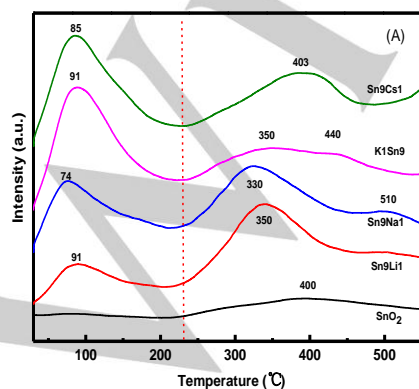
**Table 2.** Physical-chemical properties of the catalysts modified by different alkali metal oxides

Catalysts	O1s Binding Energy (eV)			$O_2^{2-}/(O_2^{2-}+O^{2-})$
	$CO_3^{2-}$	$O_2^{2-}$	$O^{2-}$	
SnO <sub>2</sub>	532.3 (OH <sup>-</sup> )	531.4	530.9	22%
Sn9Li1	532.0	531.2	530.6	35%
Sn9Na1	532.0	530.7	530.1	36%
Sn9K1	532.2	530.6	530.0	25%
Sn9Cs1	531.9	530.6	529.6	31%

To discern the relationship between the OCM reaction performance and the surface  $O_2^{2-}$  species, the  $C_2$  product yield of each catalyst is plotted versus its  $O_2^{2-}/(O_2^{2-}+O^{2-})$  molar ratio. As displayed in Figure. 3 (B), for those catalysts with better  $C_2$  yield, the surface  $O_2^{2-}$  species is generally more abundant. The un-modified SnO<sub>2</sub> possesses the smallest amount of surface  $O_2^{2-}$  species, thus displaying the lowest  $C_2$  yield. On the contrary, Sn9Li1, the sample modified by lithium oxide, possesses the largest amount of surface  $O_2^{2-}$  species, hence displaying the highest  $C_2$  yield. However, it is noticed that the  $C_2$  yield is not proportional to the relative surface  $O_2^{2-}$  amount, indicating other factors might also influence the reaction performance of the catalysts. Most probably, the surface basicity induced by the addition of different alkali metal oxides could be another reason affecting the OCM performance of the catalysts.

#### CO<sub>2</sub>-TPD analysis of the catalysts modified by different alkali metal oxides

As demonstrated previously, for an effective OCM catalyst, the presence of surface alkaline sites is necessary, which can activate the potent methane molecules.<sup>[19]</sup> Many early literatures have reported the correlations between the number of basic sites and the  $C_2$  yield in the OCM reaction.<sup>[19, 56]</sup> While all the alkaline sites are beneficial for the activation of methane molecules, the basic sites with intermediate strength are favorable for the selective formation of  $C_2$  coupling products.<sup>[3, 19]</sup> Therefore, CO<sub>2</sub>-TPD technique is adopted to probe the alteration of the surface alkaline sites of SnO<sub>2</sub> support after the modification by different alkali metal oxides, with the profiles shown in Figure. 4.

**Figure 4.** CO<sub>2</sub>-TPD profiles of the catalysts modified by different alkali metal oxides.

On the profile of individual SnO<sub>2</sub>, a broadened peak center at 400 °C is observed, indicating the presence of a small amount of alkaline sites. In contrast, with the addition of different alkaline metal oxides, the profiles of the modified catalysts become much more complicated, testifying the formation of a larger amount of alkaline sites with different strength. For clear comparison, the alkaline sites are divided into two groups according to the CO<sub>2</sub> desorption temperatures. In detail, it is defined that the CO<sub>2</sub> desorption peak below 230 °C is correspondent to weak alkaline sites and the peak above 230 °C to alkaline sites with intermediate strength (intermediate alkaline sites). The amount of weak basic sites is observed to increase in the order of SnO<sub>2</sub> < Sn9Li1 < Sn9Na1 < Sn9Cs1 < Sn9K1; and the amount of intermediate alkaline sites increases in the order of SnO<sub>2</sub> < Sn9Cs1 < Sn9K1 < Sn9Na1 < Sn9Li1.

**Table 3.** Quantified CO<sub>2</sub>-TPD results of the catalysts modified by different alkali metal oxides.

Catalysts	Weak basic sites amount (a.u.)	Intermediate basic sites amount (a.u.)	Total basic sites amount (a.u.)
SnO <sub>2</sub>	0	6	6
Sn9Li1	5	14	19
Sn9Na1	10	12	22
Sn9K1	20	9	29
Sn9Cs1	17	10	27

Although all the alkaline sites with different strength might contribute to the OCM reaction performance, the sites with intermediate strength are found relating to the selective formation of the coupling products.<sup>[3, 19, 31, 57]</sup> Therefore, the  $C_2$  yield of each catalyst is plotted versus the amount of the intermediate alkaline sites in Figure. 4 (B). It is evident that a catalyst with better  $C_2$  yield generally has a larger amount of intermediate alkaline sites, indicating the intermediate alkaline sites are critical for the formation of the coupling products. Whereas, although Sn9K1 possesses slightly larger amount of intermediate alkaline sites than Sn9Na1, it displays still evidently

lower  $C_2$  yield than Sn9Na1. The major reason is due to the presence of a larger amount of electrophilic oxygen species on the surface of Sn9Na1 (Table 2). According to these experimental facts, it is reasonable to conclude that both of the abundance of electrophilic oxygen species and intermediate alkaline sites are important for the OCM reaction. Therefore, the concerted interaction between these two types of surface active sites could determine the reaction performance of the  $SnO_2$ -based catalysts in this study. Due to the optimal concerted interaction of the two types of surface sites, Sn9Li1 displays the best reaction performance among all the catalysts modified by different alkali metal oxides, over which the highest  $C_2$  product yield around 10 % can be obtained.

### The influence of lithium oxide amount on the OCM reaction performance of the $SnO_2$ -based catalysts

With the purpose to develop catalysts having better reaction performance,  $SnO_2$ -based catalysts modified with different amounts of lithium oxide have been prepared and used for OCM reaction. As displayed in Figure. 5(A), pure  $SnO_2$  itself has very low activity for the reaction, as evidenced by the low methane conversion in the whole tested temperature region. The addition of lithium oxide improves the activity of the resulted catalysts obviously. Moreover, with the increase of the lithium oxide amount from Sn/Li molar ratio of 9/1 to 5/5, the methane conversion on the catalysts keeps on increasing. The highest activity can be obtained on Sn5Li5 catalyst. Further increasing the lithium oxide amount to Sn/Li molar ratio of 3/7 degrades the activity abruptly, implying the change of the active site property drastically. Interestingly, the  $C_2$  product selectivity of all the catalysts with different amount of lithium oxide is similar, which is around 60-70 % in the whole temperature region, and much higher than that on the pure  $SnO_2$  support, as shown in Figure. 5(B). As a result, Figure. 5 (C) exhibits that all the modified catalysts have higher  $C_2$  yield than the pure  $SnO_2$  catalyst. On Sn5Li5, the modified catalyst with a Sn/Li molar ratio of 5/5, the highest  $C_2$  yield around 15.3 % can be achieved at 750 °C. For more detailed information, the product distribution collected at different temperatures on Sn5Li5, the best catalyst in this study, is shown in Table S1.  $C_2H_4$ ,  $C_2H_6$  and  $CO_2$  are the major products. Moreover, the selectivity of  $C_2H_6$  is generally higher than that of  $C_2H_4$ . It is noted here that the similar product distribution is observed also on other catalysts in this study.

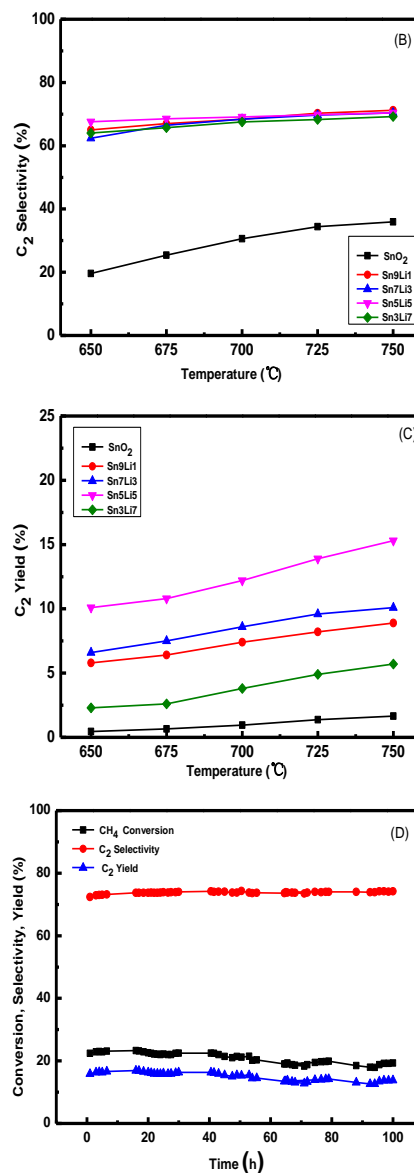
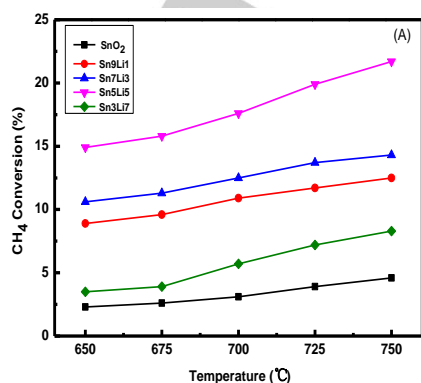


**Figure 5.** Reaction performance of the catalysts modified by different amount of lithium oxide. (A)  $CH_4$  conversion, (B)  $C_2$  product selectivity, (C)  $C_2$  product yield, (D) Stability test at 750 °C over Sn5Li5 catalyst. Reaction conditions: cat 0.2g,  $CH_4/O_2=4:1$ ,  $GHSV=18000mLh^{-1}g^{-1}$ , 50% Nitrogen balanced.

For a catalyst, the stability is an important issue to estimate its application potential. Therefore, Sn5Li5 was subjected to a 100 h stability test at 750 °C. As demonstrated in Figure. 5 (D), the methane conversion,  $C_2$  selectivity and yield are constant during the testing without any decrease, indicating this catalyst is stable for the high temperature OCM reaction.

At present,  $Mn/Na_2WO_4/SiO_2$  is still the most promising OCM catalyst for industrial application, on which the highest one way yield close to 30 % has been reported by some researchers above 800 °C.<sup>[58-59]</sup> Whereas, this catalyst has very low activity below 700 °C. To save the cost, it is always desirable to find catalysts that can be operated at lower temperatures. As compared in Figure. S3, Sn5Li5, the best catalyst in this study, displays much better reaction performance than  $Mn/Na_2WO_4/SiO_2$  catalyst under the same condition at low

temperature region. At 700 °C, the C<sub>2</sub> yield over Sn5Li5 is 12.2 % and that over Mn/Na<sub>2</sub>WO<sub>4</sub>/SiO<sub>2</sub> is only 3.0 %. It is summarized here that with the addition of appropriate amount of lithium oxide, SnO<sub>2</sub>-based catalysts with not only significantly improved reaction performance, but also very high stability can be achieved, which may give people some new thoughts on developing OCM catalysts operated at lower temperature region.

### XRD and N<sub>2</sub>-BET analysis of the catalysts modified by different amount of lithium oxide

To understand the reaction performance of the catalysts modified by different amount of lithium oxide, they were subjected to XRD analysis, with the patterns exhibited in Figure. 6. While Sn9Li1 shows still only the diffraction feature of tetragonal rutile SnO<sub>2</sub> phase, starting from Sn7Li3, a new Li<sub>2</sub>SnO<sub>3</sub> phase appears, whose amount increases with the addition amount of lithium oxide, as evidenced by the improved peak intensity of Li<sub>2</sub>SnO<sub>3</sub>. Sn7Li3 and Sn5Li5 consist of both tetragonal rutile SnO<sub>2</sub> and Li<sub>2</sub>SnO<sub>3</sub> phases. In contrast, with the further increasing of lithium oxide amount, Li<sub>2</sub>SnO<sub>3</sub> is the only detected phase for Sn3Li7 catalyst. This testifies that during the high temperature calcination process, solid phase reaction between lithium and tin oxides takes place according to the following equation:

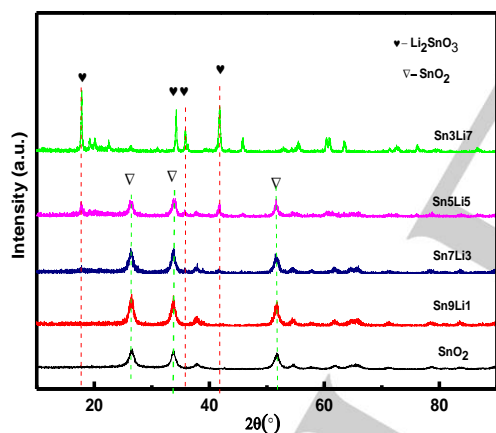
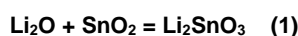


**Figure 6.** XRD patterns of the catalysts modified by different amount of lithium oxide.

Based on the stoichiometry expressed by this equation and supposing the reaction is very complete, the phase composition of the catalysts modified with different amount of lithium oxide is estimated in Table 4. Sn9Li1, Sn7Li3 and Sn5Li5 should be composed of both SnO<sub>2</sub> and Li<sub>2</sub>SnO<sub>3</sub> phases, with a theoretical SnO<sub>2</sub>/Li<sub>2</sub>SnO<sub>3</sub> molar ratio of 8.5/0.5, 5.5/1.5 and 2.5/2.5, respectively. However, Sn3Li7 should be composed of both Li<sub>2</sub>SnO<sub>3</sub> and Li<sub>2</sub>O phases with a Li<sub>2</sub>SnO<sub>3</sub>/Li<sub>2</sub>O molar ratio of 3.0/0.5. The excess Li<sub>2</sub>O is believed to be finely dispersed on the surface of Li<sub>2</sub>SnO<sub>3</sub>, thus escaping the detection by XRD.<sup>[51]</sup> Apparently, for the catalysts with both SnO<sub>2</sub> and Li<sub>2</sub>SnO<sub>3</sub> phases, the reaction performance is much better, and the best catalyst in fact consists of equal amount of the two phases. The existence

of excess amount of Li<sub>2</sub>O is actually harmful for the performance of the catalyst.

**Table 4.** Physical-chemical properties of the catalysts promoted by different amount of lithium oxide..

Sample	S <sub>BET</sub> (m <sup>2</sup> /g)	Pore volume (cm <sup>3</sup> /g)	Pore diameter (nm)	The theoretical crystalline phase composition	The actual crystalline phase composition <sup>a</sup>
SnO <sub>2</sub>	12	0.73	10.0	SnO <sub>2</sub>	SnO <sub>2</sub>
Sn9Li1	13	0.72	9.9	8.5 SnO <sub>2</sub> +0.5 Li <sub>2</sub> SnO <sub>3</sub>	SnO <sub>2</sub>
Sn7Li3	8	0.14	35.1	5.5SnO <sub>2</sub> +1.5Li <sub>2</sub> SnO <sub>3</sub>	SnO <sub>2</sub> +Li <sub>2</sub> SnO <sub>3</sub>
Sn5Li5	5	0.11	34.7	2.5SnO <sub>2</sub> +2.5Li <sub>2</sub> SnO <sub>3</sub>	SnO <sub>2</sub> +Li <sub>2</sub> SnO <sub>3</sub>
Sn3Li7	2	0.02	14.0	3Li <sub>2</sub> SnO <sub>3</sub> +0.5Li <sub>2</sub> O	Li <sub>2</sub> SnO <sub>3</sub>

a. identified by XRD.

The texture property of the catalysts modified by different amount of lithium oxide was also analyzed with N<sub>2</sub> adsorption-desorption technique. As displayed in **Figure. S4 and Table 4**, while Sn9Li1 still shows similar sorption isotherm, pore distribution profile, pore volume, pore diameter and specific surface area to the un-modified SnO<sub>2</sub>, those of Sn7Li3, Sn5Li5 and Sn3Li7 are completely different, testifying further the change of the bulk phase composition of these samples containing larger amounts of lithium oxide. With the formation of more Li<sub>2</sub>SnO<sub>3</sub> in the catalysts, the initial interparticle pores of SnO<sub>2</sub> disappear abruptly starting from Sn7Li3 catalyst. Sn3Li7, the catalyst without any SnO<sub>2</sub> and with excess Li<sub>2</sub>O possesses extra low surface area and pore volume, testifying it is nearly non-porous. Indeed, the N<sub>2</sub> adsorption-desorption results are well consistent with the XRD results, testifying the change of the bulk phase compositions of the catalysts with different amount of lithium oxide.

### Raman characterization of the catalysts modified by different amount of lithium oxide

Raman technique was used to further confirm the phase composition of the catalysts modified by different amount of lithium oxide, with the profiles exhibited in Fig. 7. For comparison, the spectroscopy of the individual SnO<sub>2</sub> was also collected, which shows three typical Raman peaks at 480, 635 and 775 cm<sup>-1</sup>, corresponding to the E<sub>g</sub>, A<sub>1g</sub> and B<sub>2g</sub> vibration modes in sequence.<sup>[60-64]</sup> While Sn9Li1 displays the same profile to pure SnO<sub>2</sub>, starting from Sn7Li3, the typical Raman peaks belonging to Li<sub>2</sub>SnO<sub>3</sub> are observed at 588, 370 and 320 cm<sup>-1</sup>,<sup>[65]</sup> whose intensities increase with the increasing amount of lithium oxide. Same to the XRD phase analysis results, in Sn7Li3 and Sn5Li5 catalysts, both of SnO<sub>2</sub> and Li<sub>2</sub>SnO<sub>3</sub> phases co-exist but with varied ratios. However, in Sn3Li7, Li<sub>2</sub>SnO<sub>3</sub> is the only detected phase. As lithium oxide is Raman silent,<sup>[66]</sup> the excess lithium oxide on this catalyst is not detectable. In brief, the Raman results are in good agreement with the XRD results, testifying the addition of different amount of lithium oxide induced the phase composition change of the catalysts, which could subsequently influence the reaction performance of the catalysts.

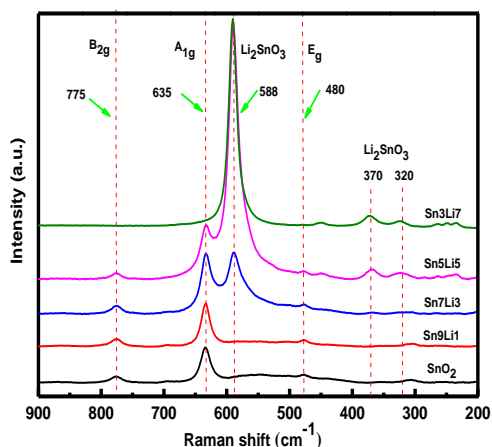


**Figure 7.** The Raman spectra of the catalysts modified by different amount of lithium oxide.

### H<sub>2</sub>-TPR study on the catalysts modified by different amount of lithium oxide

H<sub>2</sub>-TPR experiments were performed to investigate the redox property of the catalysts modified by different amount of lithium oxide, with the profiles shown in Fig. 8 and the quantified results in Table 5. Pure SnO<sub>2</sub> has a reduction peak at 653 °C, which can be assigned to the reduction of SnO<sub>2</sub> to metallic Sn.<sup>[49, 67]</sup> The quantified O/Sn atomic ratio around 2 also testifies this. With the addition of lithium oxide, this major reduction peak shifts to lower temperature gradually. However, the profile of Sn3Li7 shows no any reduction peak. As identified by XRD and Raman results above, this catalyst consists of Li<sub>2</sub>SnO<sub>3</sub> and Li<sub>2</sub>O phases. Apparently, after the formation of Li<sub>2</sub>SnO<sub>3</sub> compound, the Sn<sup>4+</sup> cations become non-reducible. Therefore, for Sn9Li1, Sn7Li3 and Sn5Li5, the observed major peak should be contributed by the reduction of the SnO<sub>2</sub> phase in the bulk. To gain deeper understanding, the H<sub>2</sub>-TPR results have been quantified and listed in Table 5. Compared with pure SnO<sub>2</sub>, the H<sub>2</sub> consumption amount based on each gram catalyst, based on each gram SnO<sub>2</sub> and the O/Sn atomic ratio decrease gradually with the increase of lithium oxide amount. Moreover, the H<sub>2</sub> consumption amount Sn3Li7, the catalyst consisting of Li<sub>2</sub>SnO<sub>3</sub> and Li<sub>2</sub>O phases, becomes zero, testifying further the Sn<sup>4+</sup> cations in the lattice of Li<sub>2</sub>SnO<sub>3</sub> compound are non-reducible.<sup>[68]</sup>

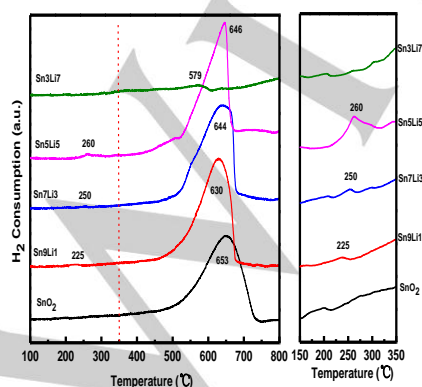


**Figure 8.** H<sub>2</sub>-TPR profiles of the catalysts modified by different amount of lithium oxide.

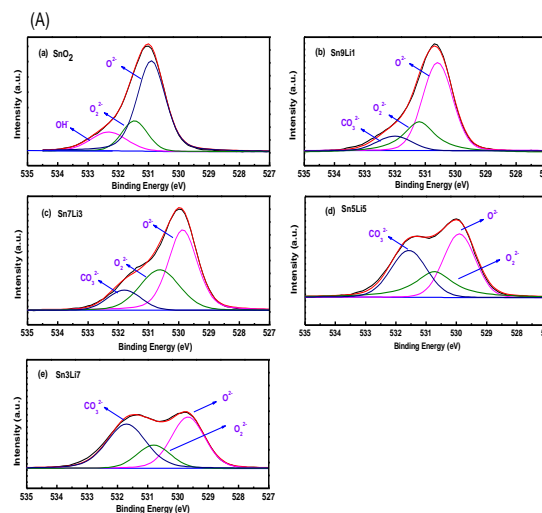
It is noted here that some of the modified catalysts show a minor reduction peak below 350 °C, as indicated by the enlarged profiles in Figure. 8. It was reported previously that as an n-type semiconductor, SnO<sub>2</sub> possesses a certain amount of deficient oxygen species,<sup>[44, 49]</sup> but which can be depleted mostly if calcined above 300 °C.<sup>[69]</sup> With the addition of appropriate amounts of lithium oxide, this deficient oxygen species is obviously stabilized at higher temperature. Therefore, on the H<sub>2</sub>-TPR profiles of Sn9Li1, Sn7Li3 and Sn5Li5, a small reduction peak corresponding to this active oxygen species can be observed. Sn5Li5, the best catalyst in this study, possesses the largest amount of this active oxygen species, as identified from the enlarged profiles. The abundance of this active surface deficient oxygen species could indeed be an important factor accounting for its outstanding OCM reaction performance.<sup>[37, 70]</sup>

**Table 5.** Quantified H<sub>2</sub>-TPR results of the catalysts modified by different amount of lithium oxide.

Catalysts	H <sub>2</sub> uptake amount above 350 °C (mmol g <sup>-1</sup> <sub>cat</sub> )	H <sub>2</sub> uptake amount above 350 °C (mmol g <sup>-1</sup> <sub>SnO<sub>2</sub>)</sub>	O/Sn atomic ratio
SnO <sub>2</sub>	13.22	13.22	1.99
Sn9Li1	12.41	12.76	1.92
Sn7Li3	11.11	12.56	1.89
Sn5Li5	10.04	11.16	1.68
Sn3Li7	0	0	0

### XPS study on the catalysts modified by different amount of lithium oxide

XPS was used again to measure the surface property of the catalysts modified by different amount of lithium oxide, with the results displayed in Figure 9 and Table 6. Figure S5 (A) exhibits the Sn 3d spectra of the catalysts. With the increasing of the added lithium oxide amount, the binding energies shift gradually to lower region, testifying the increase of electron density of the Sn cations. However, the binding energies are still typical for Sn<sup>4+</sup>, testifying that Sn is fully oxidized in the catalysts.



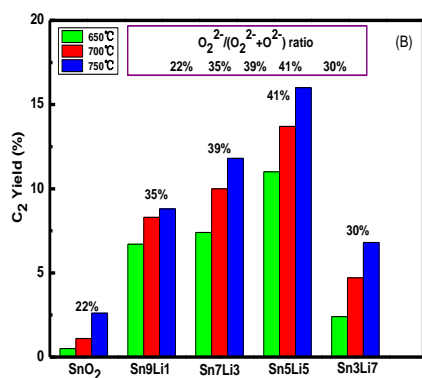


**Figure 9.** XPS analysis of the surface oxygen property for the catalysts modified by different amount of lithium oxide.

For the catalysts modified by different amount of lithium oxide, a doublet O 1s peak is still observed, as shown in Figure 9(A). Besides the major O 1s peak belonging to lattice O<sup>2-</sup> at ~530 eV, a shoulder peak assigned to loosely bond oxygen species is observed, whose area increases evidently with the increasing of lithium oxide amount. Therefore, the O1s peak of each sample is deconvoluted and quantified in Table 6. It is particularly noted that Figure S5 (B) proves that carbonate is observed for all the modified catalysts, especially those containing larger amount of lithium oxide. Therefore, when quantifying the O<sub>2</sub><sup>2-</sup>/(O<sub>2</sub><sup>2-</sup>+O<sup>2-</sup>) ratio of each catalyst, the contribution from the carbonate is subtracted. As listed in Table 6, the addition of lithium oxide improved this ratio apparently, testifying the formation of more abundant electron deficient O<sub>2</sub><sup>2-</sup> species, which is found to be important for the selective formation of the coupling products.

**Table 6.** Quantified H<sub>2</sub>-TPR results of the catalysts modified by different amount of lithium oxide.

Catalysts	O 1s Binding Energy (eV)			O <sub>2</sub> <sup>2-</sup> /(O <sub>2</sub> <sup>2-</sup> +O <sup>2-</sup> )
	CO <sub>3</sub> <sup>2-</sup>	O <sub>2</sub> <sup>2-</sup>	O <sup>2-</sup>	
SnO <sub>2</sub>	532.3	531.4	530.9	22%
Sn9Li1	532.0	531.2	530.6	35%
Sn7Li3	531.8	530.6	529.9	39%
Sn5Li5	531.6	530.7	529.9	41%
Sn3Li7	531.7	530.8	529.7	30%

To understand the relationship between the reaction performance and the surface O<sub>2</sub><sup>2-</sup> amount, the C<sub>2</sub> product yield of each catalyst is plotted versus its O<sub>2</sub><sup>2-</sup>/(O<sub>2</sub><sup>2-</sup>+O<sup>2-</sup>) molar ratio. Apparently, with the increasing of the lithium oxide from Sn9Li1 to Sn5Li5, the surface O<sub>2</sub><sup>2-</sup>/(O<sub>2</sub><sup>2-</sup>+O<sup>2-</sup>) molar ratio improves. Sn5Li5 has the highest ratio, testifying it possesses the most abundant surface electrophilic oxygen species, which explains its best performance among all the catalysts. The un-modified SnO<sub>2</sub> possesses the least amount of surface electrophilic oxygen species, thus having the lowest OCM performance among all the catalysts. It is also noticed that if a catalyst contains both of SnO<sub>2</sub> and Li<sub>2</sub>SnO<sub>3</sub> phases, it usually has a

larger amount of surface electrophilic oxygen species, thus having better reaction performance. Sn3Li7 sample, as a catalyst contains Li<sub>2</sub>SnO<sub>3</sub> phase but lacks SnO<sub>2</sub> phase, its amount of surface electrophilic oxygen species is less than other modified catalysts, thus having lower OCM reaction performance. Therefore, the presence of surface electrophilic oxygen species is important, and could be a crucial factor to decide the OCM reaction performance on the SnO<sub>2</sub>-based catalysts in this study.

#### CO<sub>2</sub>-TPD analysis of the catalysts modified by different amount of lithium oxide

As discussed above, the presence of surface alkaline sites are important for an effective OCM catalyst.<sup>[19, 33]</sup> Therefore, the influence of surface basic sites by the addition of different amount of lithium oxide has been probed by means of CO<sub>2</sub>-TPD method. As shown in **Figure 10 (A)**, both of SnO<sub>2</sub> and Sn9Li1 consist predominantly of tetragonal SnO<sub>2</sub> phase, thus they possess very small amount of surface alkaline sites. In comparison with pure SnO<sub>2</sub>, a new weak CO<sub>2</sub> desorption peak at ~90 °C is observed on the profile of Sn9Li1 catalyst. Whereas, further increasing the amount of lithium oxide obviously induces the formation of more complicated surface alkaline sites with also much larger amount. Sn7Li3 and Sn5Li5, the two catalysts composed of both large quantities of SnO<sub>2</sub> and Li<sub>2</sub>SnO<sub>3</sub> phases, display similar CO<sub>2</sub> desorption profiles, but the latter possesses evidently more abundant surface alkaline sites with intermediate strength. Sn3Li7, the catalyst containing Li<sub>2</sub>SnO<sub>3</sub> and Li<sub>2</sub>O phases, owns even more abundant and stronger alkaline sites, as evidenced by the CO<sub>2</sub> desorption peak at 528 °C

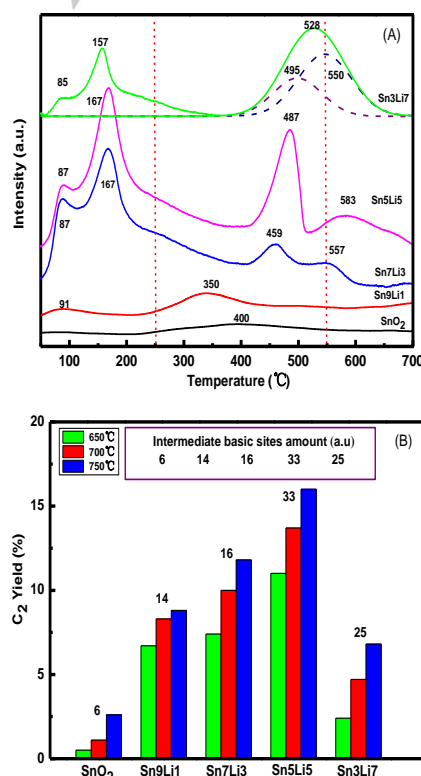


**Figure 10.** XPS analysis of the surface oxygen property for the catalysts modified by different amount of lithium oxide.

For a more accurate comparison, the alkaline sites are divided into three groups according to the CO<sub>2</sub> desorption temperatures and quantified in Table 7. In detail, it is defined that the CO<sub>2</sub> desorption peak below 250 °C is correspondent to weak alkaline sites, the peak between 250-550 °C to alkaline sites with intermediate strength (intermediate alkaline sites) and the peak above 550 °C to strong alkaline sites.<sup>[3, 31-33]</sup> While all the alkaline sites are favorable for the activation of methane molecules, the intermediate alkaline sites are important for the selective formation of coupling products.<sup>[3, 31-33]</sup> Therefore, the C<sub>2</sub> yield on the catalysts is plotted against the amount of their intermediate alkaline sites in Figure. 10(B). It is apparent that the C<sub>2</sub> product yield increases with the amount of intermediate alkaline sites, testifying that the abundance of surface intermediate alkaline sites is another factor determining the OCM reaction performance of the SnO<sub>2</sub>-based catalysts in this study.

**Table 7.** Quantified CO<sub>2</sub>-TPD results of the Catalysts modified by different amount of lithium oxide.

Catalysts	Weak basic sites amount (a.u.)	Intermediate basic sites amount (a.u.)	Total basic sites amount (a.u.)
SnO <sub>2</sub>	0	6	6
Sn9Li1	5	14	19
Sn7Li3	61	16	92
Sn5Li5	67	33	100
Sn3Li7	17	25	85

In summary, it has been disclosed in this study that for SnO<sub>2</sub>-based catalysts modified by different alkaline metal oxides, the surface electrophilic oxygen sites and intermediate alkaline sites are the two major factors influencing the OCM reaction performance. The concerted interaction of the two types of surface sites determines the reaction performance of a catalyst. As an example, Sn5Li5 possesses the most abundant two types of surface sites, thus displaying the best reaction performance among all the catalysts.

## Conclusions

With the objective to develop reactive catalysts for oxidative coupling of methane at low temperature, different alkali metal oxides have been adopted to modify the surface of SnO<sub>2</sub> with a traditional impregnation method. Since lithium oxide displays very positive modification effects, the influence of its addition amount has also been investigated and tuned. Furthermore, all the catalysts have been characterized with different techniques to study its surface and bulk property change, and correlated with the OCM reaction performance.

(1) With the addition of various alkali metal oxides, the methane conversion, C<sub>2</sub> product selectivity and yield can be significantly improved over all the modified catalysts in comparison with the un-modified SnO<sub>2</sub>. Among all the alkali metal oxides, lithium oxide shows the most positive promotion effects. XRD results have demonstrated that that tetragonal

rutile SnO<sub>2</sub> is the predominant crystalline phase for all the catalysts, and the alkali metal oxides disperse highly on the SnO<sub>2</sub> surface. As a consequence, the amounts of surface alkaline sites and electrophilic oxygen species have been evidently improved, which are believed to be the major factors influencing the OCM performance of the catalysts.

(2) By tuning the addition amount of lithium oxide, the best reaction performance can be obtained over a catalyst with a Sn/Li molar ratio of 5/5, on which 15.3 % C<sub>2</sub> yield has been achieved at 750 °C. XRD and Raman results have disclosed that for those catalysts with evident improved OCM reaction performance, the co-existence of both SnO<sub>2</sub> and Li<sub>2</sub>SnO<sub>3</sub> phases is necessary and important. The best catalyst consists of equal amounts of these two phases.

(3) Based on the results achieved over the catalysts modified by different amount of lithium oxide, it has been discovered that the C<sub>2</sub> yield at different temperatures is proportional to the amount of both surface intermediate alkaline sites and electrophilic oxygen species. Therefore, it is concluded that the abundance and the concerted interaction of these two types of surface active sites are the major factors determining the OCM reaction performance of the SnO<sub>2</sub>-based catalysts in this study.

(4) Last but not the least, the optimized catalyst, Sn5Li5, which has a Sn/Li molar ratio of 5/5 and consists equal amount of SnO<sub>2</sub> and Li<sub>2</sub>SnO<sub>3</sub> phases, exhibits much better reaction performance than Mn/Na<sub>2</sub>WO<sub>4</sub>/SiO<sub>2</sub>, the most promising OCM catalyst at present, at low temperature region (below 750 °C), and its reaction performance is very stable. Therefore, we trust information provided here may give people some new enlightenment on how to develop novel OCM catalysts that can be operated at low temperature and facilitate the industrialization process of this important chemical engineering reaction.

## Experimental Section

### Catalyst preparation

The SnO<sub>2</sub> supports were prepared by Precipitation method. In detail, 0.05 mol SnCl<sub>4</sub>·5H<sub>2</sub>O (A.R.) was dissolved into a certain amount of distilled deionized (DDI) water to form stable solution. Then NH<sub>3</sub>·H<sub>2</sub>O (25%-28 wt. %) aqueous solution was added dropwise into it until the pH reached 7. Afterwards the precipitate was vacuum filtered and washed thoroughly with DDI water until Cl free, with a total dissolved solid (TDS) less than 10 ppm. The resultant precipitate was dried at 120 °C for 12 h, and then calcined at 800 °C for 4 h in air atmosphere and ground into powder, which is named SnO<sub>2</sub>.

The supported alkali metal oxide catalysts were prepared by a traditional impregnation method with aqueous nitrate solution as their precursor. With Li-modified catalyst as an example, LiNO<sub>3</sub> (A.R.) was first dissolved into DDI water to prepare a stable aqueous solution (0.5 mol·L<sup>-1</sup>). Afterwards, a certain amount of SnO<sub>2</sub> support prepared in the last step was added into this LiNO<sub>3</sub> solution. The mixture was then dried at 120 °C for 12 h and calcined again at 800 °C with a heating rate of 2 °C·min<sup>-1</sup> in air atmosphere for 4 hours to get the final catalyst, which was named Sn9Li1 according to the Sn/Li molar ratio. For the preparation of the catalysts modified with other alkali metal oxides having the same molar ratios, the same procedure was used except that NaNO<sub>3</sub> (A.R.), KNO<sub>3</sub> (A.R.) and CsNO<sub>3</sub> (A.R.) solutions were used as the precursors. The catalysts are named Sn9Li1, Sn9Na1, Sn9K and Sn9Cs1. For the preparation of the catalysts modified with different amount of lithium

oxide, the same procedure was used and the catalysts are named Sn7Li3, Sn5Li5 and Sn3Li7 according to the Sn/Li molar ratios.

### Catalyst characterization

The bulk phase composition of the fresh catalysts were examined by using a Bruker AXS D8Focus diffractometer (XRD) that was operated at 40 kV and 30 mA with a Cu target and  $K\alpha$ -ray irradiation. The Scans were collected over a  $2\theta$  range from  $10^\circ$  to  $90^\circ$  with step of  $2^\circ \text{ min}^{-1}$ .

Nitrogen adsorption-desorption experiments of the all samples were performed at 77 K on ASAP2020 instrument. The specific surface areas of the catalysts were calculated using the Brunauer-Emmett-Teller (BET) method in the relative pressure ( $P/P_0$ ) range of 0.05-0.25. The pore size distribution of samples was calculated with the Barrett-Joyner-Halenda (BJH) method and the average pore sizes of the samples were obtained from the peak positions of the distribution curves.

Hydrogen temperature programmed reduction ( $\text{H}_2$ -TPR) experiments were carried out on a FINESORB 3010C system equipped with a thermal conductivity detector (TCD). 10 mg catalyst was loaded and pretreated in a high purity  $\text{N}_2$  stream at  $120^\circ\text{C}$  for 0.5 h to remove any surface impurities. After that the hydrogen temperature-programmed reduction was started from room temperature to  $800^\circ\text{C}$  at a rate of  $10^\circ\text{C}/\text{min}$  in a 30 mL/min 10%  $\text{H}_2/\text{Ar}$  gas mixture flow. The  $\text{H}_2$  consumption was quantified by using CuO (99.99%) as the calibration standard sample.

$\text{CO}_2$  temperature programmed desorption ( $\text{CO}_2$ -TPD) was carried out with a micromeritics Auto Chem 2920 apparatus. Typically, 50 mg catalyst was used for the test in a  $30 \text{ ml min}^{-1}$  He flow. Prior to the test, the sample was heated to  $400^\circ\text{C}$  and kept for 30 min to remove any possible impurities. Afterwards, the sample was cooled down to  $50^\circ\text{C}$  and exposed to a  $30 \text{ ml min}^{-1}$   $\text{CO}_2$  flow for 1 h to saturate the surface completely, which was followed by purging with a  $30 \text{ ml min}^{-1}$  ultra-high purity He flow to remove the any physically absorbed  $\text{CO}_2$  for 30 min. After all these pretreatments, the catalyst was heated from  $50$  to  $600^\circ\text{C}$  at a rate of  $10^\circ\text{C min}^{-1}$ .

Raman spectra of the catalysts were measured using excitation wavelength of 514 nm in Renishaw in Via instrument. The measured Raman shift range is from  $200$ - $1000 \text{ cm}^{-1}$ .

X-ray photoelectron spectroscopy (XPS) experiments were performed on a PerkinElmer PHI1600 system equipped with a single Mg-K-X-ray source operating at 300 W and 15 kV of voltage. The spectra were recorded at ambient temperature with an ultrahigh vacuum. The binding energies of the catalysts were calibrated by using the C 1s peak of graphite at  $284.6 \text{ eV}$  as a standard.

### Activity evaluation

The performance of the catalysts was assessed in a fixed-bed quartz reactor with an inner diameter of 10 mm at 1 atm. 200 mg catalyst was placed into the quartz reactor tube. The reaction feed is composed of 40% methane, 10% oxygen and 50% nitrogen balance, which results into a volume proportion of methane/oxygen of 4/1. The total flow rate of the reactant mixture is  $60 \text{ mL}\cdot\text{min}^{-1}$  with a gas hourly space velocity (GHSV) of  $18000 \text{ mL}\cdot\text{h}^{-1}\cdot\text{g}^{-1}$ . The methane coupling products were analyzed by two online gas chromatographs, with a GC9310 chromatograph equipped with a TDX-01 column and a TCD detector for monitoring CO,  $\text{CO}_2$  and  $\text{CH}_4$ ; and a GC9310II chromatograph equipped with a Propak Q column and a FID detector for monitoring  $\text{CH}_4$ ,  $\text{C}_2\text{H}_6$ ,  $\text{C}_2\text{H}_4$ ,  $\text{C}_3\text{H}_8$ ,  $\text{C}_3\text{H}_6$ . For a detailed evaluation process, a measurement starts from  $650^\circ\text{C}$  and then the temperature increases by a  $25^\circ\text{C}$  gap until  $750^\circ\text{C}$ . All measurements were taken after 1 h stabilization after reaching the target temperature to ensure steady state kinetic data.

The methane conversion ( $X_{\text{CH}_4}$ ),  $\text{C}_2$  selectivity ( $S_{\text{C}_2}$ ) and  $\text{C}_2$  yield ( $Y_{\text{C}_2}$ ) in this study are calculated with the following equations:

$$X_{\text{CH}_4} = \frac{\text{CO} + \text{CO}_2 + 2(\text{C}_2\text{H}_4 + \text{C}_2\text{H}_6) + 3(\text{C}_3\text{H}_6 + \text{C}_3\text{H}_8)}{(\text{CH}_4)_{\text{in}}} \times 100\% \quad (2)$$

$$S_{\text{C}_2} = \frac{2(\text{C}_2\text{H}_4 + \text{C}_2\text{H}_6)}{\text{CO} + \text{CO}_2 + 2(\text{C}_2\text{H}_4 + \text{C}_2\text{H}_6) + 3(\text{C}_3\text{H}_6 + \text{C}_3\text{H}_8)} \times 100\% \quad (3)$$

$$Y_{\text{C}_2} = X_{\text{CH}_4} \cdot S_{\text{C}_2} \times 100\% \quad (4)$$

### Acknowledgements

*This work is supported by the Natural Science Foundation of China (21567016, 21566022, 21666020), the Natural Science Foundation of Jiangxi Province (20171BAB213013, 20151BBE50006), the Education Department of Jiangxi Province (GJJ150016, GJJ150085, KJLD14005), and the Graduate Student Creativity Funding of Jiangxi Province (YC2016-S004) which are greatly acknowledged by the authors..*

**Keywords:** oxidative coupling of methane • alkali metal oxides •  $\text{SnO}_2$  catalysts • electrophilic oxygen sites • intermediate alkaline sites

- [1] A. Holmen, *Catalysis Today* 2009, 142, 2-8.
- [2] J. H. Lunsford, *Catalysis Today* 2000, 63, 165-174.
- [3] Z. Wang, G. Zou, X. Luo, H. Liu, R. Gao, L. Chou, X. Wang, *Journal of Natural Gas Chemistry* 2012, 21, 49-55.
- [4] X. Guo, G. Fang, G. Li, H. Ma, H. Fan, L. Yu, C. Ma, X. Wu, D. Deng, M. Wei, D. Tan, R. Si, S. Zhang, J. Li, L. Sun, Z. Tang, X. Pan, X. Bao, *Science* 2014, 344, 616-619.
- [5] J.-Z. Zhang, M. A. Long, R. F. Howe, *Catalysis today* 1998, 44, 293-300.
- [6] G. Keller, M. Bhasin, *Journal of Catalysis* 1982, 73, 9-19.
- [7] J. H. Lunsford, *Angewandte Chemie International Edition in English* 1995, 34, 970-980.
- [8] G. Klunkhammer, M. Bender, R. Weiss, J. Lupton, *Nature* 1985, 314, 25.
- [9] S. Sarsani, D. West, W. Liang, V. Balakotaiah, *Chemical Engineering Journal* 2017, 328, 484-496.
- [10] A. Aseem, G. G. Jeba, M. T. Conato, J. D. Rimer, M. P. Harold, *Chemical Engineering Journal* 2018, 331, 132-143.
- [11] J. S. Lee, S. Oyama, *Catalysis Reviews Science and Engineering* 1988, 30, 249-280.
- [12] E. N. VOSKRESENSKAYA, V. G. ROGULEVA, A. G. ANSHITS, *Catalysis Reviews* 1995, 37, 101-143.
- [13] G. Ertl, H. Knözinger, F. Schüth, J. Weitkamp, *Handbook of heterogeneous catalysis: 8 volumes*, wiley-vch, 2008.
- [14] U. Zavyalova, M. Holena, R. Schlögl, M. Baerns, *ChemCatChem* 2011, 3, 1935-1947.
- [15] C. Hammond, S. Conrad, I. Hermans, *ChemSusChem* 2012, 5, 1668-1686.
- [16] D. J. Driscoll, W. Martir, J.-X. Wang, J. H. Lunsford, *J. Am. Chem. Soc. (United States)* 1985, 107.
- [17] T. Ito, J. H. Lunsford, *Nature* 1985, 314, 721-722.
- [18] N. A. S. Amin, S. E. Pheng, *Chemical Engineering Journal* 2006, 116, 187-195.
- [19] T. W. Elkins, S. J. Roberts, H. E. Hagelin-Weaver, *Applied Catalysis A: General* 2016, 528, 175-190.
- [20] L. Tang, D. Yamaguchi, L. Wong, N. Burke, K. Chiang, *Catalysis Today* 2011, 178, 172-180.
- [21] K. Nagaoka, T. Karasuda, K.-i. Aika, *Journal of Catalysis* 1999, 181, 160-164.

- [22] S. Arndt, U. Simon, K. Kiefer, T. Otremba, K. Siemensmeyer, M. Wollgarten, A. Berthold, F. Schmidt, O. Görke, R. Schomäcker, K.-P. Dinse, *ChemCatChem* 2017, 9, 3583-3596.
- [23] U. Simon, S. Alarcón Villaseca, H. Shang, S. V. Levchenko, S. Arndt, J. D. Epping, O. Görke, M. Scheffler, R. Schomäcker, J. van Tol, A. Ozarowski, K.-P. Dinse, *ChemCatChem* 2017, 9, 3597-3610.
- [24] L. Chou, Y. Cai, B. Zhang, J. Niu, S. Ji, S. Li, *Applied Catalysis A: General* 2003, 238, 185-191.
- [25] T. W. Elkins, H. E. Hagelin-Weaver, *Applied Catalysis A: General* 2015, 497, 96-106.
- [26] T. Serres, C. Aquino, C. Mirodatos, Y. Schuurman, *Applied Catalysis A: General* 2015, 504, 509-518.
- [27] J. Wang, L. Chou, B. Zhang, H. Song, J. Zhao, J. Yang, S. Li, *Journal of Molecular Catalysis A: Chemical* 2006, 245, 272-277.
- [28] J. Wang, L. Chou, B. Zhang, H. Song, J. Yang, J. Zhao, S. Li, *Catalysis Communications* 2006, 7, 59-63.
- [29] Z. Zhang, S. Ji, *Computers & Chemical Engineering* 2016, 90, 247-259.
- [30] S. Ji, T. Xiao, S. Li, L. Chou, B. Zhang, C. Xu, R. Hou, A. P. E. York, M. L. H. Green, *Journal of Catalysis* 2003, 220, 47-56.
- [31] P. Huang, Y. Zhao, J. Zhang, Y. Zhu, Y. Sun, *Nanoscale* 2013, 5, 10844-10848.
- [32] T. Jiang, J. Song, M. Huo, N. Yang, J. Liu, J. Zhang, Y. Sun, Y. Zhu, *RSC Adv.* 2016, 6, 34872-34876.
- [33] F. Papa, P. Luminita, P. Osiceanu, R. Birjega, M. Akane, I. Balint, *Journal of Molecular Catalysis A: Chemical* 2011, 346, 46-54.
- [34] V. J. Ferreira, P. Tavares, J. L. Figueiredo, J. L. Faria, *Catalysis Communications* 2013, 42, 50-53.
- [35] T. W. Elkins, H. E. Hagelin-Weaver, *Applied Catalysis A: General* 2015, 497, 96-106.
- [36] P. Wang, G. Zhao, Y. Wang, Y. Lu, *Science Advances* 2017, 3, e1603180.
- [37] V. J. Ferreira, P. Tavares, J. L. Figueiredo, J. L. Faria, *Industrial & Engineering Chemistry Research* 2012, 51, 10535-10541.
- [38] S. Arndt, G. Laugel, S. Levchenko, R. Horn, M. Baerns, M. Scheffler, R. Schlögl, R. Schomäcker, *Catalysis Reviews* 2011, 53, 424-514.
- [39] X. Wang, Y.-C. Xie, *Applied Catalysis B: Environmental* 2001, 35, 85-94.
- [40] C. Liu, H. Xian, Z. Jiang, L. Wang, J. Zhang, L. Zheng, Y. Tan, X. Li, *Applied Catalysis B: Environmental* 2015, 176, 542-552.
- [41] C. Gao, S. Yuan, B. Cao, J. Yu, *Chemical Engineering Journal* 2017, 325, 378-385.
- [42] H. Xu, Z. Qu, S. Zhao, D. Yue, W. Huang, N. Yan, *Chemical Engineering Journal* 2016, 292, 123-129.
- [43] J. Yu, D. Zhao, X. Xu, X. Wang, N. Zhang, *ChemCatChem* 2012, 4, 1122-1132.
- [44] R. Sasikala, N. Gupta, S. Kulshreshtha, *Catalysis letters* 2001, 71, 69-73.
- [45] G. Croft, M. Fuller, *Nature* 1977, 269, 585-586.
- [46] H. Widjaja, K. Sekizawa, K. Eguchi, *Bulletin of the Chemical Society of Japan* 1999, 72, 313-320.
- [47] K. Sekizawa, H. Widjaja, S. Maeda, Y. Ozawa, K. Eguchi, *Applied Catalysis A: General* 2000, 200, 211-217.
- [48] S. Chai, X. Bai, J. Li, C. Liu, T. Ding, Y. Tian, C. Liu, H. Xian, W. Mi, X. Li, *Applied Surface Science* 2017, 402, 12-20.
- [49] X. Xu, F. Liu, X. Han, Y. Wu, W. Liu, R. Zhang, N. Zhang, X. Wang, *Catal. Sci. Technol.* 2016, 6, 5280-5291.
- [50] X. Xu, R. Zhang, X. Zeng, X. Han, Y. Li, Y. Liu, X. Wang, *ChemCatChem* 2013, 5, 2025-2036.
- [51] Y.-C. Xie, Y.-Q. Tang, *Advances in catalysis* 1990, 37, 1-43.
- [52] H. Wang, F. Sun, Y. Zhang, L. Li, H. Chen, Q. Wu, J. C. Yu, *Journal of Materials Chemistry* 2010, 20, 5641.
- [53] G. Choi, L. Satyanarayana, J. Park, *Applied Surface Science* 2006, 252, 7878-7883.
- [54] H. Ma, K. Teng, Y. Fu, Y. Song, Y. Wang, X. Dong, *Energy & Environmental Science* 2011, 4, 3067.
- [55] S. Gubbala, H. B. Russell, H. Shah, B. Deb, J. Jasinski, H. Rypkema, M. K. Sunkara, *Energy & Environmental Science* 2009, 2, 1302.
- [56] A. Davydov, M. Shepotko, A. Budneva, *Catalysis today* 1995, 24, 225-230.
- [57] V. Choudhary, V. Rane, *Journal of Catalysis* 1991, 130, 411-422.
- [58] R. Ghose, H. T. Hwang, A. Varma, *Applied Catalysis A: General* 2014, 472, 39-46.
- [59] S. Ji, *Journal of Catalysis* 2003, 220, 47-56.
- [60] W. Wang, C. Xu, G. Wang, Y. Liu, C. Zheng, *Journal of Applied Physics* 2002, 92, 2740-2742.
- [61] M. N. Rumyantseva, A. M. Gaskov, N. Rosman, T. Pagnier, J. R. Morante, *Chemistry of materials* 2005, 17, 893-901.
- [62] L. Z. Liu, X. L. Wu, F. Gao, J. C. Shen, T. H. Li, P. K. Chu, *Solid State Communications* 2011, 151, 811-814.
- [63] A. Kar, S. Kundu, A. Patra, *The Journal of Physical Chemistry C* 2010, 115, 118-124.
- [64] M. Epifani, J. D. Prades, E. Comini, E. Pellicer, M. Avella, P. Siciliano, G. Faglia, A. Cirera, R. Scotti, F. Morazzoni, *The Journal of Physical Chemistry C* 2008, 112, 19540-19546.
- [65] Z. Fu, P. Liu, J. Ma, B. Guo, X. Chen, H. Zhang, *Materials Research Bulletin* 2016, 77, 78-83.
- [66] K. Kunc, I. Loa, A. Grzechnik, K. Syassen, *physica status solidi (b)* 2005, 242, 1857-1863.
- [67] X. Wang, L. Xiao, H. Peng, W. Liu, X. Xu, *J. Mater. Chem. A* 2014, 2, 5616-5619.
- [68] Y. Huang, G. Wang, T. Wu, S. Peng, *JOURNAL OF NATURAL GAS CHEMISTRY* 1998, 7, 102-107.
- [69] M. A. Mäki-Jaskari, T. T. Rantala, *Physical Review B* 2002, 65, 245428.
- [70] A. J. Nagy, G. Mestl, R. Schlögl, *Journal of Catalysis* 1999, 188, 58-68.

## Entry for the Table of Contents (Please choose one layout)

Layout 1:

## FULL PAPER

**Lithium oxide boosts:** Due to the balance between  $\text{SnO}_2$  and  $\text{Li}_2\text{SnO}_3$  phases, both the amounts of surface active oxygen and alkaline sites have been increased, thus improving significantly the low temperature activity and  $\text{C}_2$  product yield for methane oxidative coupling.



Liang Peng,[a] Junwei Xu,[a] Xiuzhong Fang,[a] Wenming Liu,[a] Xianglan Xu,[a] Liang Liu,[a] Zhongchen Li,[a] Honggen Peng,[a] Renyang Zheng,[b] Xiang Wang\*[a]

Page No. – Page No.

**$\text{SnO}_2$ -based catalysts with superior low temperature performance for oxidative coupling of methane: insight into the promotional effects of alkali metal oxides**